

pubs.acs.org/acsapm Article

Effects of Trace Water on Self-Assembly of Sulfonated Block Copolymers During Solution Processing

Karthika Madathil, Kayla A. Lantz, Morgan Stefik,* and Gila E. Stein*



Cite This: ACS Appl. Polym. Mater. 2020, 2, 4893-4901



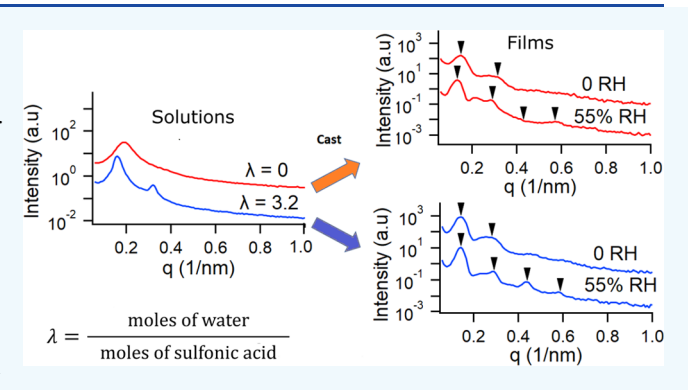
ACCESS

Metrics & More

Article Recommendations

s Supporting Information

ABSTRACT: Solution-cast films of sulfonated block copolymers are investigated for applications in water purification, gas separations, and fuel cells. It is well known that solvent composition influences the structures that form in solutions of sulfonated block copolymers and in the corresponding films. The solutions often contain trace water due to the hygroscopic nature of sulfonated polymers, and the effect of trace water on structure formation has not been previously explored. Water will drive dissociation of sulfonic acid, which in turn might accelerate the rearrangement of polymer chains by disrupting hydrogen bonds between acid groups. In this work, we examine the effects of trace water on the solution-state structure of a sulfonated pentablock copolymer (SPC) and the ultimate film morphology using small-



angle X-ray scattering. The solvent used was a mixture of toluene and n-propanol with varying molar ratios of water to sulfonic acid (λ). In solutions with $\lambda = 0$, the SPC adopts a disordered structure. The addition of trace water ($\lambda = 3.2$) to SPC solutions drives a rapid self-assembly into an ordered lamellar structure. However, the presence of trace water in the solution has little effect on processing the SPC into films as water will rapidly escape from the drying film in a dry environment. For film processing, ambient humidity is more important than trace water in the solution as moisture in air provides a constant supply of water to the film as the solvent evaporates. While there are many variables that control the morphology of solution-cast SPC films, these studies demonstrate that trace amounts of water play a critical role in kinetics and thermodynamics of solution-state self-assembly and the evolution of nanoscale structures during film drying.

KEYWORDS: Nexar, sulfonated block copolymer, lamellar self-assembly, solution processing, acid dissociation

■ INTRODUCTION

Block copolymers (BCPs) are an interesting class of materials due to their ability to self-assemble into well-defined nanoscale structures in the melt state and in solutions. In the melt state, the equilibrium phase behavior is controlled by several factors, including (1) enthalpic incompatibility between the blocks, controlled by χN , where χ is the the Flory-Huggins interaction parameter between two blocks and N is the degree of polymerization; (2) the volume fraction of each block; and (3) the architecture of the block copolymer. However, block copolymers with highly incompatible blocks have very slow diffusion rates in melts,2 which makes it difficult to achieve equilibrium microphase-separated morphologies by thermal annealing. Consequently, solvent-based processing is often used for such systems, and the resulting morphologies are often different from the equilibrium state produced by melt processing.

Solution processing is commonly used for preparing membranes based on ionic block copolymer films for fuel cells,^{3–7} gas separations^{8,9} and water purification.^{10–12} In these block copolymers, one of the blocks contains ionic or acidic

moieties, which provide transport pathways for water, protons, and ions, while the other neutral block (or blocks) is used to tailor mechanical properties. The lamellar (LAM) morphology has been extensively studied for applications in membranes. The transport properties in this phase depend on various factors such as grain sizes and defect structures, which are controlled by relative volumes of each block, ^{13,14} the type of solvent used in processing, ^{17,18} and other process-related conditions such as thermal history. Highly defective LAM structures are similar to network-like phases and provide improved transport properties. ^{14,16,17,19} Furthermore, the LAM morphology occupies the largest fraction of the block copolymer phase diagram, so it is not very sensitive to changes in the relative volume fractions of each block due to missed

Received: July 24, 2020 Accepted: August 31, 2020 Published: August 31, 2020





targets in synthesis or swelling by solvents. In solvent processing, there are numerous variables that determine the morphology of the final dry film, including solvent selectivity toward each block, polymer concentration in solution and solvent evaporation rate. A major challenge with solution-cast ionic block copolymers is understanding how these process variables will influence the film morphology.

In this work, we studied the effects of trace water on selfassembly of a sulfonated pentablock copolymer (SPC), poly(tert-butylstyrene-b-hydrogenated isoprene-b-sulfonated styrene-b-hydrogenated isoprene-b-tert-butylstyrene) (tBS-HI-SS-HI-tBS). The solution-state self-assembly of this SPC has been studied in prior works, and depending on the polymer concentration and solvent polarity, the SPC can either dissolve into free chains or assemble into spheres, lamellae, and disordered nanoscale aggregates. ^{17,20–23} The structures of solution-cast SPC films have also been studied, and morphologies such as lamellae, cylinders, and spheres have been observed depending on the solvent type used for casting. 17,24-27 Trace water is difficult to avoid during the solution processing of SPC into films as the material soaks up water when stored at ambient humidity due to the hygroscopic sulfonated midblock.^{21,28} As a result, the solution will contain small amounts of water (ca. 1-5 wt %) unless the polymer is dried prior to dissolution or the solution is dried prior to use. However, to our knowledge, the effects of trace water on solution-state SPC self-assembly and subsequent processing into films have not been previously considered. In polyelectrolytes with strong interactions arising from intrinsic ion pairs, water provides mobility to the polymer chains by increasing the free volume and acting as a lubricant between the chains.² This effect of water results in plasticization of polyelectrolyte films as a function of relative humidity. 30-35 In sulfonated polymers, the presence of water drives the dissociation of sulfonic acid groups,³⁶ resulting in a similar plasticizing behavior. Therefore, the enhanced mobility of polymer chains arising from the dissociation of sulfonic acid likely impacts the kinetics of SPC self-assembly in solution and the morphology that forms during subsequent film processing.

For the purposes of this work, trace water refers to molar ratios of water to sulfonic acid (λ) in the range of $\lambda = 0 - 3.2$, corresponding to water compositions of 0-1.9 wt % relative to the solvent. The investigation was split into two parts: First, the self-assembly of SPC in solution was monitored with timeresolved small-angle X-ray scattering (SAXS) as a function of λ . Second, the structure of solution-cast films was measured with SAXS as a function of λ in the solution, relative humidity during casting, and evaporation rate/casting method. These studies show that kinetics of solution-state self-assembly is accelerated in proportion to λ , but film formation is not very sensitive to λ and is largely determined by other process conditions such as evaporation rate and humidity.

EXPERIMENTAL SECTION

SPC Material. The SPC (tBS-HI-SS-HI-tBS) was provided by Kraton Polymers as films (Figure 1).37 The midblock styrene was sulfonated to 52 mol %. The weight fractions of the SPC blocks were 20-10-40-10-20 (tBS-HI-SS-HI-tBS) and the overall molecular weight was approximately 60–70 kg/mol. The as-received films had a spherical SPC morphology with an SS core, as reported by others²⁸, and confirmed with SAXS measurements. The films were soaked in deionized water (18.2 M Ω) for 24 h to extract byproducts from the sulfonation reaction and then dried in air for 24 h.

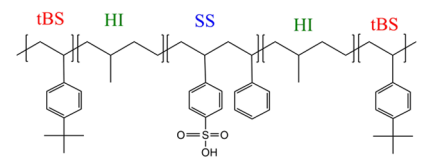


Figure 1. Structure of BCP, where tBS = tert-butylstyrene, HI = hydrogenated isoprene, and SS = partially sulfonated styrene (52 mol %). Molecular weight (pre-sulfonation): 15-10-28-10-15 kg/mol.

Polymer Solution Preparation for Time-Resolved SAXS. Toluene (T, ACS grade, Fisher) and 1-propanol (nP, ≥99.0%, VWR) were dried at room temperature by storage over 30% w/v of molecular sieves (3Å, 8–12 mesh, Acros Organics) for 1 week.³⁸ The SPC was dried in a vacuum oven at 80 °C for 24 h. The polymer mass was determined immediately after drying, and the material was stored under continuous vacuum while solvent mixtures were prepared. Unless otherwise indicated, all solvent mixtures were prepared with a 33:67 ratio of nP/T (wt/wt) denoted as nP₃₃:T₆₇. The amount of water required to produce λ of 1.6 or 3.2 was calculated for the measured mass of the dry polymer and then added to the solvent mixture. The SPC composition in solution was 16 wt % in all cases. These solutions were tightly sealed and left undisturbed for 24 h to undergo complete dissolution.

Film Formation at Low and High Humidity. All solutions were prepared and stored inside a nitrogen purged glovebox to avoid exposure to water. Solvent vials containing nP, T, and water were taken into a glovebox after purging the head space with argon. SPC films were loaded into a glovebox immediately after drying. Two solutions were prepared with $\lambda = 0$ and $\lambda = 3.2$, each containing 16 wt % polymer by mass and nP₃₃:T₆₇ solvent. Films were drop-cast both in the glovebox (maintained below 3 ppm H₂O) as well as under ambient humidity. Drop-casting was done on Kapton sheets inside a balance using 0.1 mL of solution that was aged for a specified time between 1-25 days. The mass was recorded as a function of time during the evaporation process, and the solvent evaporation with time is shown in Figure S1. For drop-casting in ambient humidity, a small amount of solution was drawn from the stock solution in the glovebox and taken in a sealed vial. The thicknesses of drop-cast films (after solvent removal) were between 150-300 μ m. Film preparation for studies on the effect of the evaporation rate/casting method was done by bar-coating on Kapton at ambient humidity using an Elcometer film applicator with gap heights ranging from 125-1125 μ m. The thicknesses of bar-coated films (after solvent evaporation) were between $10-100 \mu m$.

Small-Angle X-ray Scattering (SAXS). Time-resolved SAXS measurements of solutions were performed with a SAXSLab Ganesha at the University of South Carolina SAXS Collaborative. An 80 µL quantity of each solution was placed in a hermetically sealed sandwich cell with Kapton windows and stored under continuous vacuum maintained at 10^{-2} mbar throughout the 15 days of measurement to prevent the ingress of extraneous water. A Xenocs GeniX 3D microfocus source with a copper target was used to produce a monochromatic beam with a 0.154 nm wavelength. The sample to detector distance was 1 m. A Pilatus 300 k detector (Dectris) was used to collect the 2D scattering patterns with nominal pixel dimensions of 172 μ m × 172 μ m. The data acquisition time was 30 min. All static measurements of solutions and dry films were performed at the Polymer Characterization Laboratory at the University of Tennessee, Knoxville. A Xenocs GeniX 3D microfocus source with a copper target was used to produce a monochromatic beam with a 0.154 nm wavelength. The sample to detector distance was 0.9 m for films and 1.8 m for solutions. A Pilatus3 R 300 K detector (Dectris) was used with nominal pixel dimensions of 172 μ m \times 172 μ m. The data acquisition time was 3 min for films and 10 min for solutions. The two-dimensional images from each measurement (either instrument) were azimuthally integrated with SAXSGUI to yield a one-dimensional scattering profile of intensity I (a.u) versus

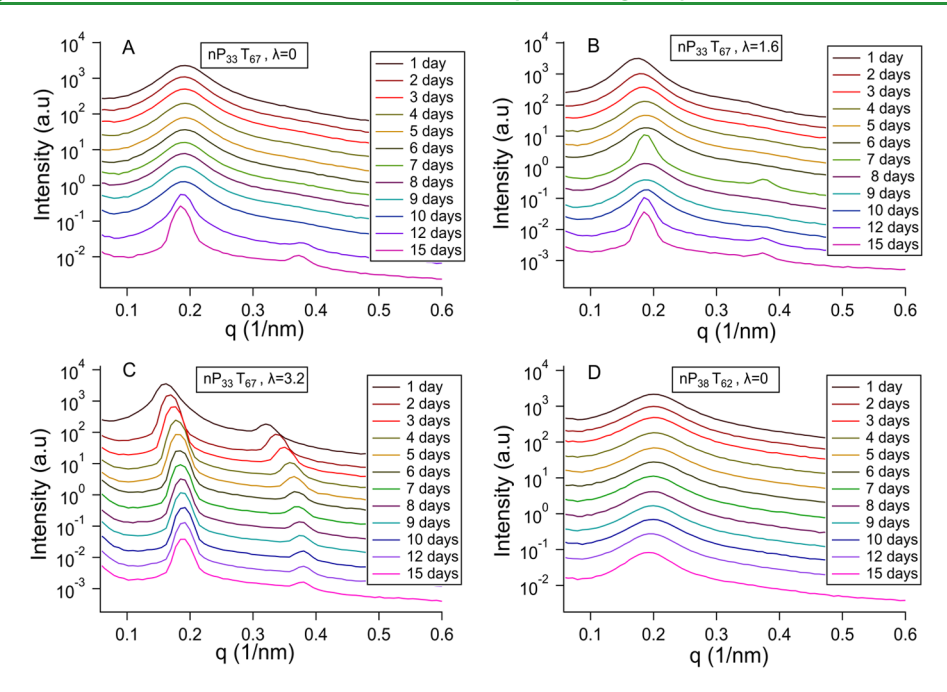


Figure 2. Time-resolved SAXS measurements of 16 wt % SPC solutions in different solvent mixtures: (A) nP_{33} : T_{67} , $\lambda = 0$; (B) nP_{33} : T_{67} , $\lambda = 1.6$; (C) nP_{33} : T_{67} , $\lambda = 3.2$; (D) nP_{38} : T_{62} , nP/T, $\lambda = 0$.

scattering vector q (nm⁻¹). In all the figures showing SAXS data, the plots from each data set have been offset vertically for clarity.

Transmission Electron Microscopy (TEM). TEM measurements were performed on drop-cast films that were sectioned to a thickness of around 30 nm by a Leica EM FC7 microtome at -30 °C. The sections were stained by sealing them in a centrifuge tube for 30 min with osmium tetroxide vapor, which segregates in HI and may reactively stain tBS. The obtained sample slices were imaged by a Zeiss Libra 200 HT FE MC transmission electron microscope.

RESULTS AND DISCUSSIONS

Solution Structure. The solution phase behavior of this SPC in polar, nonpolar, and mixed solvents has been studied in previous works. $^{17,20-23}$ When the solution composition is 4–5 wt % polymer, the SPC structure is spherical micelles with an SS core 21,22 at low solvent polarity and changes to free chains 21 or inverted micelles with an SS corona 21 with increasing polarity of the solvent. In one of these examples, the SPC was dried before dissolving in the solvent, 21 but the other study did not specify the water content.²² As polymer loading in the solvent is increased, the SPC can assemble into either ordered or disordered morphologies, depending on the solvent composition. For example, when the SPC is dissolved in nP/ T solvent mixtures at a loading of 20 wt %, which includes 20 wt % water from storage at ambient humidity, the structure after 2 days of dissolution at room temperature is lamellar (LAM) for 29-36 wt % nP and disordered (DIS) for 40-50 wt % nP.1

Building on these prior results, the first goal of the present study is to examine the kinetics of SPC self-assembly in nP/T solvent mixtures with and without trace water. For this purpose, we selected conditions that produce a LAM phase in solution as this morphology is of particular interest for membranes. Unless otherwise stated, the solvent used for these studies was nP₃₃:T₆₇ (33 wt % nP, 67 wt % T) and the SPC loading in the solvent was 16 wt %. The molar ratio of water to sulfonic acid (λ) was varied in the range of 0 to 3.2. These

conditions fall within the LAM region of the solution phase diagram at room temperature. 17

Figure 2 reports time-resolved SAXS data for solutions at room temperature with different amounts of trace water over a period of 15 days. The position of the primary peak (q^*) and its full width at half-maximum (FWHM) were determined by fitting to a Voigt line shape. Figure 2A shows data for the nP₃₃:T₆₇ solvent with $\lambda = 0$. From 1–10 days, the SAXS spectra exhibit a single broad peak at $q^* = 0.19 \text{ nm}^{-1}$ (FWHM = 0.055 nm⁻¹), indicative of a poorly ordered structure. By day 12, the q^* peak becomes narrower (FWHM = 0.027 nm⁻¹) and a higher-order peak emerges at $2q^*$, consistent with the formation of an ordered LAM structure. According to the Scherrer equation, grain size is proportional to 1/FWHM, so the grain size approximately doubles over this time frame.

The time-resolved SAXS data were collected from solutions in tightly sealed sandwich cells that were stored under vacuum over 15 days. To ensure that the transition from a poorly ordered structure to ordered LAM was not induced by a leak in the cell, i.e., an undetectable level of solvent evaporation under the dynamic vacuum, several control experiments were implemented using solutions that were aged in sealed vials at ambient pressure for different aging times. These control experiments agree with the time-resolved studies in Figure 2A and confirm a transition from a poorly ordered structure at shorter times (1, 5, and 11 days) to ordered LAM at longer times (21 days) when aged at room temperature (Figure S2).

The effect of water on SPC self-assembly was studied by adding trace amounts of water to the nP_{33} : T_{67} solvent mixture. Figure 2B shows time-resolved data for solutions with $\lambda=1.6$, corresponding with 0.9 wt % water in the solvent, and the results are similar to solutions with $\lambda=0$. The initial structure is poorly ordered, as evidenced by a single broad peak at $q^*=0.17~\rm nm^{-1}$ (FWHM = 0.051 nm⁻¹). By day 12, the q^* peak is sharper (FWHM = 0.019 nm⁻¹) and a higher-order peak is observed at $2q^*$ consistent with the formation of an ordered LAM phase. A second-order peak is also observed on day 7 for

this sample, which then disappears by day 8 and re-emerges by day 12. This behavior was not observed for the experiments with $\lambda=0$ or $\lambda=3.2$ samples, which were repeated with consistent results, and the cause of this re-emergent behavior is unknown. Figure 2C shows time-resolved data for solutions with $\lambda=3.2$, corresponding with 1.9 wt % water in the solvent. The SPC ordered into the LAM phase within 1 day, as evidenced by narrow peaks at $q^*=0.16$ nm⁻¹ (FWHM = 0.029 nm⁻¹) and $2q^*$. We also studied the solution structure for a solution with $\lambda=8.7$ aged for 1 day, corresponding with 5.3 wt % water in the solvent, which showed LAM ordering with narrow peaks at $q^*=0.14$ nm⁻¹ (FWHM = 0.025 nm⁻¹) and $2q^*$. These data are included in Figure S3.

In solutions containing trace water, the primary and higher-order peaks shift to larger q as a function of time (Figure 2B,C). Figure S4 shows that the initial domain periodicity $d=2\pi/q^*$ (at day 1) is swollen in proportion to water content. The domain periodicity remains constant with time in dry solutions, but in solutions with trace water, the domain periodicity decreases with time and converges with that of the dry solutions by day 15. This effect is only observed for solutions that were stored under vacuum for the 15 day duration of the measurement and was not reproduced in control experiments where the solutions were aged in sealed vials at ambient pressure (Figure S2). Thus, for solutions prepared with trace water and stored under vacuum, the reduction in domain spacing as a function of time is likely an effect of water evaporation.

The data in Figure 2A-C demonstrate that water can accelerate the self-assembly kinetics in solution. However, it is unclear if this effect is associated with the chemistry of water rather than an increase in the solvent polarity. To test this point, an nP_{38} : T_{62} solvent mixture with $\lambda = 0$ was prepared. As shown in the Supporting Information (Table S1), the Hansen solubility parameter of this mixture is approximately equal to that of nP_{33} : T_{67} with $\lambda = 3.2$. Figure 2D reports the timeresolved SAXS data for this solvent mixture. From day 1 through day 15, the spectra show a single broad peak at $q^* =$ 0.12 nm^{-1} , similar to the data shown in Figure 2A for nP₃₃:T₆₇ with $\lambda = 0$. Therefore, we conclude that the accelerated kinetics of self-assembly is specific to the chemistry of water rather than changes in solvent polarity. In the absence of water, intermolecular hydrogen bonding between sulfonic acid moieties could hinder rearrangement of the polymer chains and trap poorly ordered morphologies in the solution. With the addition of trace water to the solvent, the sulfonic acid can dissociate and provide the chains the mobility to rearrange into ordered structures. In hydrated films of sulfonated polymers, including SPC²⁸ and Nafion, 40 infrared absorbance spectroscopy has been used to confirm the dissociation of sulfonic acid. While SAXS cannot detect sulfonic acid dissociation, the domain periodicity increases in proportion to λ (Table 1 and Figure S3), providing indirect evidence that water is taken up by the SPC morphology.

To further substantiate the role of water in the solution phase self-assembly, we studied the change in solution-state structure when water is added to a dry nP_{33} : T_{67} solution (λ = 0) with a disordered SPC structure. All solutions were aged at ambient pressure in sealed vials to avoid the complications of potential water/solvent evaporation. Figure 3 reports the SAXS data for these studies. The data labeled "dry solution" were acquired after aging for 1 day and show a single broad peak at q*=0.19 nm^{-1} (FWHM = 0.055 nm^{-1}) that corresponds with

Table 1. Summary of Solution-State Structure as a Function of Solvent Composition and Trace Water Content a

| nP/T | λ | $q^* (nm^{-1})$ | d (nm) | FWHM (nm ⁻¹) |
|-------|-----|-----------------|--------|--------------------------|
| 33:67 | 0 | 0.19 | 33 | 0.055 |
| 33:67 | 1.6 | 0.17 | 36 | 0.051 |
| 33:67 | 3.2 | 0.16 | 39 | 0.029 |
| 33:67 | 8.7 | 0.14 | 44 | 0.025 |
| 38:62 | 0 | 0.20 | 31 | 0.068 |

"Solutions were aged for 1 day at room temperature. The position of the primary scattering peak is q^* , the SPC domain periodicity (or correlation length scale) is $d = 2\pi/q^*$, and FWHM is the full width at half-maximum of the primary scattering peak.

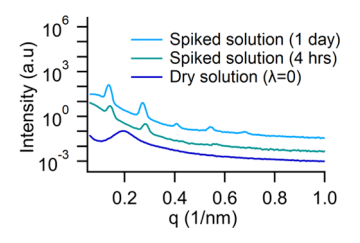


Figure 3. SAXS data for a dry solution with 16 wt % SPC in nP/T solvent mixture (33:67) and after "spiking" with water ($\lambda = 3.2$) and aging for 4 h and 1 day.

a domain periodicity of d=33 nm. The data labeled "spiked solution" were acquired after the addition of water to achieve $\lambda=3.2$. SAXS data recorded 4 h after spiking with water showed two well-defined peaks at $q^*=0.142$ nm⁻¹ (FWHM = 0.022 nm⁻¹) and $2q^*$, consistent with a LAM structure having a domain periodicity of d=44 nm. After aging the spiked solution for a full day, the SAXS data show a primary scattering peak at $q^*=0.134$ nm⁻¹ (FWHM = 0.019 nm⁻¹) and four higher-order peaks at $2q^*$, $3q^*$, $4q^*$, and $5q^*$, consistent with a well-ordered LAM structure with domain periodicity of d=47 nm.

The SAXS data in Figures 2C and 3 were both acquired from solutions with nP_{33} : T_{67} and $\lambda = 3.2$, and the preparation differs only in regard to when water was added to the solution. For both cases, a LAM structure is observed within 1 day after the addition of water. However, the "water spiking" process produces a larger domain size and better order (more higher-order peaks) than mixing all constituents in a single step. This suggests that water is more readily taken up by the sulfonated domains when it is added after an initial SPC dissolution step.

Film Structure. Previous works have examined the morphologies of solution-cast SPC films as a function of sulfonation level (26-52 mol %), solvent composition/ polarity, and loading of SPC in the solution. 17,24-27 When the solutions are prepared with 2-2.5 wt % SPC in nonpolar solvents, such as cyclohexane, cyclohexane/heptane, toluene with low amounts of isopropanol, or cyclohexane/heptane with low amounts of tetrahydrofuran (THF), the resulting films have SS-rich domains in a tBS/HI matrix.²⁴⁻²⁶ This film structure appears to be partly templated by the solution-state structure, i.e., spherical micelles with an SS core and tBS/HI corona, as discussed in the preceding section. The arrangement of the SS domains in the films is influenced by the solvent composition. As an example, when films are cast from mixtures of cyclohexane/heptane/THF, the connectivity of the SS domains increases with the amount of THF. 26 When the solutions are prepared with 2-2.5 wt % SPC in moderately

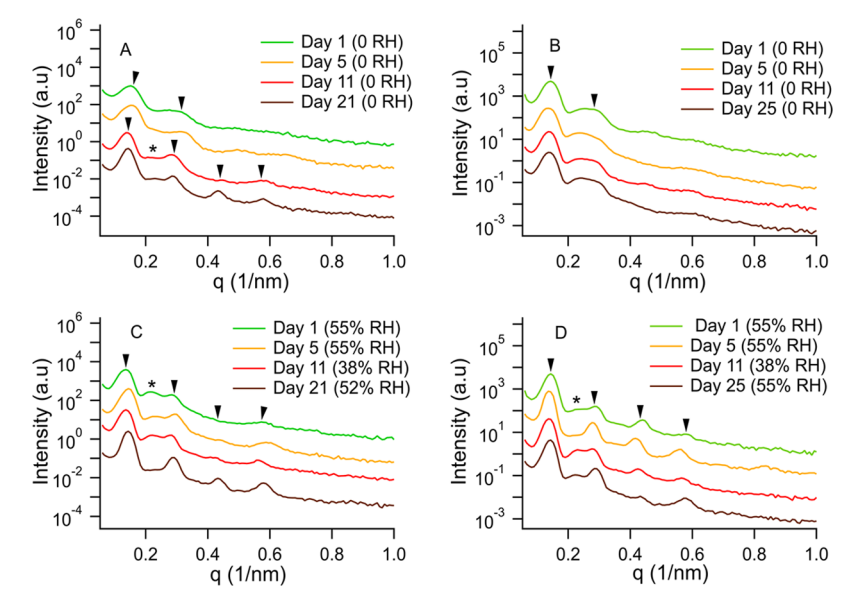


Figure 4. SAXS data for films produced by drop-casting at (A, B) near-zero relative humidity or (C, D) ambient relative humidity. Films were cast from (A, C) dry solutions and (B, D) solutions containing trace amounts of water. The inverted triangles correspond to LAM peak positions, and the "asterisk" corresponds to the peak resulting from the minor HEX phase.

polar solvents, such as THF, the resulting films can have coexisting LAM and hexagonally packed cylinders (HEX) morphologies with the sulfonated midblock forming the continuous matrix. For films cast from 16 wt % SPC in nP/T mixed solvents, a transition from LAM to network-like morphologies is observed with increasing nP content. These LAM and network-like morphologies in films are produced from LAM and disordered structures in solution, respectively.

These findings suggest that the structure of the solvent-cast SPC films is correlated with the preassembled solution structure. However, the final film morphology of solution-cast block copolymer films is also controlled by structural transitions during the casting process. 41–44 In the specific case of polyelectrolyte-based block copolymers, trace water might influence the film formation process by disrupting intermolecular hydrogen bonding, as shown in the previous section for SPC in solution. To interrogate this point, we examined the film morphology as a function of λ in the casting solvent, ambient humidity during casting, and solvent evaporation rate.

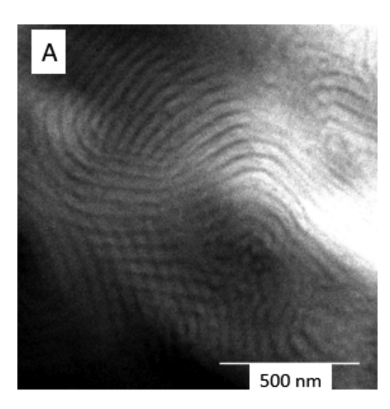
Figure 4 shows the SAXS data of films that were prepared by drop-casting from dry solutions ($\lambda=0$) and solutions with trace water ($\lambda=3.2$). The solutions were aged for 1–25 days prior to casting. The relative humidity (RH) during drop-casting was either near zero or ambient (38–55%). The evaporation rate was similar for all the drop-cast films (Figure S1) at approximately 4 mg/min for the first 10 min, followed by a continuously reduced rate until the films were dry.

Dry solutions aged for 1-5 days have a disordered structure with periodicity d=33 nm (Figure 2A), and the corresponding films prepared by drop-casting at near-zero RH have a poorly ordered LAM structure with d=42 nm: the SAXS data have a primary peak at $q^*=0.15$ nm⁻¹ with a broad secondary peak at $2q^*$ (Figure 4A). Dry solutions aged for more than 11 days have a LAM structure with d=34 nm (Figure 2A), and the corresponding films prepared by drop-casting at near-zero RH have a LAM structure with d=45 nm: the SAXS data have a primary peak at $q^*=0.14$ nm⁻¹ and higher-order peaks at $2q^*$, $3q^*$, and $4q^*$ (Figure 4A). We note that the lamellar domain periodicity in films was always larger than that in solutions,

which demonstrates that the nP/T mixture is a poor quality solvent for the SPC polymer and drives the collapse of the chains. In films, the FWHM of the q^* peak is approximately 0.048 nm⁻¹ when cast from solutions aged for 1–5 days and is reduced to 0.034 nm⁻¹ when cast from solutions aged longer than 11 days.

The SPC solutions with trace water show an ordered LAM structure that does not change with aging time (Figure 2C). SAXS measurements of the corresponding films cast at 0% RH have a scattering peak at $q^* = 0.14$ nm⁻¹, as well as a broad hump at higher q that appears to be the convolution of two peaks near $\sqrt{3} q^*$ and $2q^*$ (Figure 4B). These data are not consistent with a pure LAM or cylindrical phase: scattering from LAM will produce peak ratios of 1:2:3, while scattering from hexagonally packed cylinders will produce peak ratios of 1: $\sqrt{3}$:2. As TEM images of films cast from the 11 day aged solution show a mixture of "line" and "dot" domains (Figure 5A), the SAXS data likely reflect a mixture of LAM and cylindrical phases. The FWHM of the q^* peak in films is independent of the solution aging time and is approximately 0.04 nm⁻¹, which is higher than observed in the solutions with trace water (0.029 nm⁻¹ for $\lambda = 3.2$). These data show that adding water to the solution does not produce films with a well-ordered LAM structure if the casting is done at zero humidity. In the previous section, we noted that trace water will escape from solutions in a "sealed" cell when stored under vacuum, presumably due to a small leak in the cell. Therefore, we propose that water rapidly escapes from the wet film when cast at 0% RH. As a result, hydrogen bonds between sulfonic acid groups may inhibit the necessary chain rearrangements to maintain an ordered LAM structure as the film dries.

To examine the role of ambient humidity in film formation, a series of films were cast from solutions with and without trace water at 38–55% RH. SAXS data show an ordered LAM structure in all films, irrespective of the trace water content or aging time of the solution, as evidenced by scattering peaks at $q^* \approx 0.0136 \text{ nm}^{-1}$ and $2q^*$, $3q^*$, and $4q^*$ (Figure 4C,D). The relative peak intensities are different among the films, and in particular, there are several data sets in Figure 4C where the



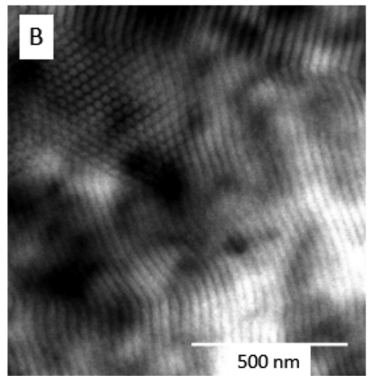


Figure 5. TEM images of drop-cast films. (A) Day 11 (0% RH) from Figure 4C. (B) Day 11 (38% RH) from Figure 4D. The bright regions correspond to the SS domains, and the dark regions correspond to the tBS/HI domains after staining with osmium tetroxide.

intensity of the $3q^*$ peak is very weak. Relative peak intensities are largely controlled by the form factor of the domains, i.e., the size and shape, so differences among the films could be explained by variations in water uptake and domain swelling. The SAXS data for most of the films show an additional peak at $q=0.23~\mathrm{nm}^{-1}$, between q^* and $2q^*$, which is marked with a "*" in Figure 4A,C,D. A TEM image for one of these cases, a film cast at 38% RH from a solution with trace water that was aged for 11 days, is consistent with a predominantly LAM structure and a minor cylindrical phase (Figure 5B). The minor HEX phase is likely due to changes in solution composition as the solvent evaporates. 41,43

All of the films develop a LAM structure, with evidence of a minor cylindrical phase in some cases, irrespective of trace water content, solution aging time, or relative humidity during film casting. The SAXS data for films processed under ambient humidity show at least four scattering peaks, indicative of a well-ordered LAM structure. In contrast, most of the SAXS data for films processed under dry conditions show few higherorder peaks. Furthermore, the FWHM of the primary SAXS peak is lower for films cast at ambient humidity as compared to films cast at 0% RH, which indicates that a humid environment produces a better defined LAM morphology than a dry environment. The TEM images are consistent with these observations: films cast under dry conditions develop a more tortuous, "fingerprint"-like LAM structure (Figure 5A), while films cast under humid conditions develop large ordered grains (Figure 5B). In order to understand how quickly the polymer can take up water under humid conditions, the increase in mass of a dry SPC film was recorded as a function of time at 38 and 55% RH. From Figure S1, we can see that the timescale for water uptake by the dry polymer is comparable to the timescale of solvent evaporation. Therefore, a humid processing environment might facilitate the organization of a more ordered LAM phase by supplying water to the film as the organic solvents evaporate.

The effect of solvent evaporation rate on the final film structure was qualitatively examined by comparing dropcasting and bar-coating processing methods. The solution used for casting was prepared by adding trace water (to achieve λ = 3.2) to a well-dissolved solution of 16 wt % SPC in nP₃₂:T₆₇ solvent and then aging the solution for 1 day to obtain a highly ordered LAM morphology. This approach is shown in Figure 3, where spiking an initially dry solution with water drove a rapid transition from a poorly ordered structure to the ordered LAM state. The time required for drying was varied through bar-coating with a range of gap heights. The gap height controls the initial thickness and therefore volume of the wet film, so increasing the gap increases the drying time. We note that drying times could not be directly measured during barcoating, but visual inspection of the drying films confirmed the expected trend. The film cast with the smallest gap height appeared dry within seconds of casting, whereas the film cast with the largest gap height took several minutes to dry. In comparison, all the drop-cast films stayed wet for 10-15 min. Figure 6 shows the SAXS data for these bar-coated films as a

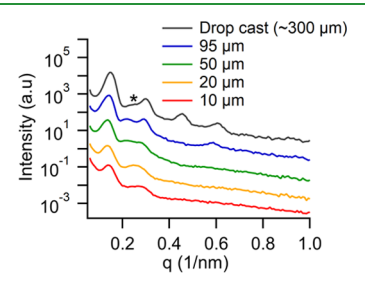


Figure 6. SAXS data for bar-coated films with different gap heights. The legend reports the dry film thickness, which is proportional to the initial wet film thickness.

function of final film thickness, as well as a drop-cast film for comparison (slowest evaporation rate). As the initial thickness of the wet film increases, producing longer drying times, a minor cylindrical phase emerges (marked by the *). The FWHM of the first-order scattering peak is in the range of 0.036–0.039 nm⁻¹ for the thin bar-coated films and 0.032 nm⁻¹ for the thick drop-cast films, which demonstrates that long drying times can improve lamellar order. Conversely, with the shortest drying times, the lamellar order is poorly developed and the formation of a minor HEX phase is suppressed.

The production of films with poorly ordered LAM from the fast evaporation of solutions with well-ordered LAM seems counter-intuitive as one might expect that fast evaporation would trap the ordered solution-state structure. However, the drying of the solution-cast film is a complex process: the film thickness contracts and the domain periodicity expands as solvent evaporates, and these processes likely disrupt the LAM ordering. When evaporation takes longer time, the chains have more time to rearrange into an ordered LAM structure.

Finally, another way to control the structure of solution-cast films is through sequential deposition of layers. When a new layer is deposited, solvent can diffuse into the underlying dry film and provide the mobility for rearrangements into a new structure. Figure 7 shows SAXS data for single-layer and four-layer films. The solution was prepared by adding trace water

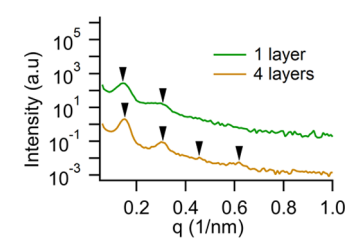


Figure 7. SAXS data for single-layer and four-layer bar-coated films.

(to achieve $\lambda = 3.2$) to a well-dissolved solution of 16 wt % SPC in nP₃₃:T₆₇ solvent and then aging the solution for 1 day to obtain a highly ordered LAM morphology. Films were cast by bar-coating with a gap height of 125 μ m. The dry thicknesses of the single-layer and four-layer films were 20 μ m and 65 μ m, respectively. The SAXS data for the single-layer film show a primary peak at $q^* = 0.14 \text{ nm}^{-1}$ (FWHM = 0.047 nm⁻¹) and a second broad peak at $2q^*$, consistent with a poorly ordered LAM structure. The SAXS data for the fourlayer film show a primary peak at $q^* = 0.15 \text{ nm}^{-1}$ (FWHM = 0.033 nm^{-1}) and higher-order peaks at $2q^*$, $3q^*$, and $4q^*$, consistent with a well-ordered LAM structure. There are no signs of a minor cylindrical phase in either film. The process of sequentially depositing layers is similar to a direct immersion annealing process, wherein a polymer film is immersed in a marginal solvent that swells the polymer, imparting mobility to the chains for rearrangement without dissolving the entire film.⁴⁵ With the immersion annealing process, the ordering of domains improved with increased immersion time. Sequential deposition of new layers increases the solvent exposure time of the previous layers, and therefore, the results are similar to increasing the immersion annealing time.

CONCLUSIONS

We examined the effects of trace water on self-assembly of an SPC in solution and on the morphology of solution-cast SPC films. The SPC was dissolved at 16 wt % in a nP₃₃:T₆₇ solvent, and the molar ratio of water to sulfonic acid was varied from λ = 0 up to λ = 3.2. The structures in solutions and in films were characterized by SAXS. In a dry solution, the SPC structure slowly evolves from a disordered state to ordered LAM over a period of approximately 10 days. With the addition of trace water to the solvent $(\lambda > 0)$, the domain periodicity swelled in proportion to water content, demonstrating that the SPC takes up water. In solutions with $\lambda \gtrsim 3.2$, an ordered LAM structure was achieved within 1 day. The accelerated kinetics with trace water are attributed to dissociation of sulfonic acid, which likely increases the chain mobility by disrupting hydrogen bonds between acid groups. The addition of controlled amounts of water could thus be a potential technique to accelerate self-assembly kinetics and facilitate ordering in solutions of polyelectrolyte-based BCPs.

The amount of trace water in the solution was found to have little impact on the ultimate morphology of SPC films, but ambient humidity during processing did play a role. These points were demonstrated by examining the morphology of SPC films that were cast at either ~0% RH or ambient humidity from solutions with and without trace water. At ~0% RH, the SPC assembled into poorly ordered LAM irrespective

of water content in the casting solution. This outcome is explained by the escape of water from the solvent to the dry atmosphere during the early stages of film drying. In contrast, when films were cast at ambient humidity from solutions with or without trace water, the ultimate morphology was wellordered LAM. This effect is attributed to the uptake of environmental water by the wet film. In addition to ambient humidity, the final film structure is also influenced by the time taken for the solvent to evaporate. Longer drying time leads to ordered LAM with a minor cylindrical phase, while shorter drying time traps a disordered LAM structure. These different outcomes are partly attributable to the timescales for water uptake by the SPC as more water can be taken up by the SPC as evaporation rate is reduced. These findings demonstrate that water content offers a simple means to tune ordering kinetics during solution-casting of sulfonated block copolymers, providing access to both ordered and disordered morphologies. This may be useful in the design of SPC membranes as poorly ordered LAM provide better transport pathways than wellordered LAM. 14,16,17,19

ASSOCIATED CONTENT

Supporting Information

The Supporting Information is available free of charge at https://pubs.acs.org/doi/10.1021/acsapm.0c00806.

Solvent evaporation rate for solution casting, time-resolved solution SAXS data for control experiment, solution SAXS data for solutions with different λ aged for 1 day, change in domain spacing with time for solutions stored in vacuum, and solubility parameters for mixed solvents and interaction distance between mixed solvents and polymer blocks (PDF)

AUTHOR INFORMATION

Corresponding Authors

Morgan Stefik — Department of Chemistry and Biochemistry, University of South Carolina, Columbia, South Carolina 29208, United States; Email: stefik@mailbox.sc.edu

Gila E. Stein — Department of Chemical and Biomolecular Engineering, The University of Tennessee at Knoxville, Knoxville, Tennessee 37996, United States; Occid.org/0000-

Authors

Karthika Madathil — Department of Chemical and Biomolecular Engineering, The University of Tennessee at Knoxville, Knoxville, Tennessee 37996, United States; orcid.org/0000-0002-9128-0786

0002-3973-4496; Email: gstein4@utk.edu

Kayla A. Lantz – Department of Chemistry and Biochemistry, University of South Carolina, Columbia, South Carolina 29208, United States

Complete contact information is available at: https://pubs.acs.org/10.1021/acsapm.0c00806

Notes

The authors declare no competing financial interest.

ACKNOWLEDGMENTS

K.M. and G.E.S. acknowledge partial financial support from Kraton Corporation and from the National Science Foundation (NSF) award no. DMR-1905487. K.A.L. acknowledges support by the NSF Established Program to Stimulate

Competitive Research (EPSCoR) Program, NSF award no. OIA-1655740. M.S. acknowledges support by the NSF CAREER program, NSF award no. DMR-1752615. This research used facilities at the Polymer Characterization Laboratory and the Microscopy Laboratory of the Joint Institute for Advanced Materials (JIAM) at the University of Tennessee, Knoxville. We thank John Dunlap for assistance with TEM. SAXS measurements at the University of Tennessee, Knoxville were enabled by the Major Research Instrumentation program of the NSF under award no. DMR-1827474. This work also made use of the South Carolina SAXS Collaborative.

REFERENCES

- (1) Bates, F. S.; Fredrickson, G. H. Block Copolymer Thermodynamics: Theory and Experiment. *Annu. Rev. Phys. Chem.* **1990**, 525–557
- (2) Yokoyama, H. Diffusion of block copolymers. *Mater. Sci. Eng., R* **2006**, 53, 199–248.
- (3) Meier-Haack, J.; Taeger, A.; Vogel, C.; Schlenstedt, K.; Lenk, W.; Lehmann, D. Membranes from sulfonated block copolymers for use in fuel cells. *Sep. Purif. Technol.* **2005**, *41*, 207–220.
- (4) Bae, B.; Hoshi, T.; Miyatake, K.; Watanabe, M. Sulfonated block poly(arylene ether sulfone) membranes for fuel cell applications via oligomeric sulfonation. *Macromolecules* **2011**, *44*, 3884–3892.
- (5) Bae, B.; Miyatake, K.; Watanabe, M. Synthesis and properties of sulfonated block copolymers having fluorenyl groups for fuel-cell applications. ACS Appl. Mater. Interfaces 2009, 1, 1279–1286.
- (6) Elabd, Y. A.; Walker, C. W.; Beyer, F. L. Triblock copolymer ionomer membranes: Part II. Structure characterization and its effects on transport properties and direct methanol fuel cell performance. *J. Membr. Sci.* **2004**, *231*, 181–188.
- (7) Lwoya, B. S.; Albert, J. N. L. Nanostructured Block Copolymers for Proton Exchange Membrane Fuel Cells. *Energy Environ. Focus* **2015**, *4*, 278–290.
- (8) Fan, Y.; Zhang, M.; Moore, R. B.; Lee, H. S.; McGrath, J. E.; Cornelius, C. J. Viscoelastic and gas transport properties of a series of multiblock copolymer ionomers. *Polymer* **2011**, *52*, 3963–3969.
- (9) Fan, Y.; Zhang, M.; Moore, R. B.; Cornelius, C. J. Structure, physical properties, and molecule transport of gas, liquid, and ions within a pentablock copolymer. *J. Membr. Sci.* **2014**, *464*, 179–187.
- (10) Geise, G. M.; Freeman, B. D.; Paul, D. R. Characterization of a sulfonated pentablock copolymer for desalination applications. *Polymer* **2010**, *51*, 5815–5822.
- (11) Wang, Q.; Lu, Y.; Li, N. Preparation, characterization and performance of sulfonated poly(styrene-ethylene/butylene-styrene) block copolymer membranes for water desalination by pervaporation. *Desalination* **2016**, 390, 33–46.
- (12) Thomas, E. R.; Jain, A.; Mann, S. C.; Yang, Y.; Green, M. D.; Walker, W. S.; Perreault, F.; Lind, M. L.; Verduzco, R. Freestanding self-assembled sulfonated pentablock terpolymer membranes for high flux pervaporation desalination. *J. Membr. Sci.* **2020**, 118460.
- (13) Campbell, I. P.; Lau, G. J.; Feaver, J. L.; Stoykovich, M. P. Network connectivity and long-range continuity of lamellar morphologies in block copolymer thin films. *Macromolecules* **2012**, 45, 1587–1594.
- (14) Arges, C. G.; Kambe, Y.; Dolejsi, M.; Wu, G.-P.; Segal-Pertz, T.; Ren, J.; Cao, C.; Craig, G. S. W.; Nealey, P. F. Interconnected ionic domains enhance conductivity in microphase separated block copolymer electrolytes. *J. Mater. Chem. A* **2017**, *5*, 5619–5629.
- (15) Sanoja, G. E.; Popere, B. C.; Beckingham, B. S.; Evans, C. M.; Lynd, N. A.; Segalman, R. A. Structure-Conductivity Relationships of Block Copolymer Membranes Based on Hydrated Protic Polymerized Ionic Liquids: Effect of Domain Spacing. *Macromolecules* **2016**, *49*, 2216–2223.
- (16) Chintapalli, M.; Chen, X. C.; Thelen, J. L.; Teran, A. A.; Wang, X.; Garetz, B. A.; Balsara, N. P. Effect of grain size on the ionic

- conductivity of a block copolymer electrolyte. *Macromolecules* **2014**, 47, 5424–5431.
- (17) Truong, P. V.; Black, R. L.; Coote, J. P.; Lee, B.; Ardebili, H.; Stein, G. E. Systematic Approaches To Tailor the Morphologies and Transport Properties of Solution-Cast Sulfonated Pentablock Copolymers. ACS Appl. Polym. Mater. 2019, 1, 8–17.
- (18) Campbell, I. P.; He, C.; Stoykovich, M. P. Topologically distinct lamellar block copolymer morphologies formed by solvent and thermal annealing. *ACS Macro Lett.* **2013**, *2*, 918–923.
- (19) Diederichsen, K. M.; Brow, R. R.; Stoykovich, M. P. Percolating transport and the conductive scaling relationship in lamellar block copolymers under confinement. *ACS Nano* **2015**, *9*, 2465–2476.
- (20) Choi, J. H.; Kota, A.; Winey, K. I. Micellar morphology in sulfonated pentablock copolymer solutions. *Ind. Eng. Chem. Res.* **2010**, 49, 12093–12097.
- (21) Griffin, P. J.; Salmon, G. B.; Ford, J.; Winey, K. I. Predicting the solution morphology of a sulfonated pentablock copolymer in binary solvent mixtures. *J. Polym. Sci., Part B: Polym. Phys.* **2016**, *54*, 254–262.
- (22) Mineart, K. P.; Ryan, J. J.; Appavou, M. S.; Lee, B.; Gradzielski, M.; Spontak, R. J. Self-Assembly of a Midblock-Sulfonated Pentablock Copolymer in Mixed Organic Solvents: A Combined SAXS and SANS Analysis. *Langmuir* **2019**, *35*, 1032–1039.
- (23) Etampawala, T. N.; Aryal, D.; Osti, N. C.; He, L.; Heller, W. T.; Willis, C. L.; Grest, G. S.; Perahia, D. Association of a multifunctional ionic block copolymer in a selective solvent. *J. Chem. Phys.* **2016**, *145*, 184903.
- (24) Mineart, K. P.; Jiang, X.; Jinnai, H.; Takahara, A.; Spontak, R. J. Morphological investigation of midblock-sulfonated block ionomers prepared from solvents differing in polarity. *Macromol. Rapid Commun.* **2015**, *36*, 432–438.
- (25) Wang, D.; Fan, Y. F.; Zhang, M.; Moore, R. B.; Cornelius, C. J. Ionomer solution to film solidification dependence upon solvent type and its impact upon morphology and ion transport. *Eur. Polym. J.* **2017**, *97*, 169–177.
- (26) Zheng, W.; Cornelius, C. J. Solvent tunable multi-block ionomer morphology and its relationship to modulus, water swelling, directionally dependent ion transport, and actuator performance. *Polymer* **2016**, *103*, 104–111.
- (27) Jain, A.; Weathers, C.; Kim, J.; Meyer, M. D.; Walker, W. S.; Li, Q.; Verduzco, R. Self assembled, sulfonated pentablock copolymer cation exchange coatings for membrane capacitive deionization. *Molecular Systems Design and Engineering* **2019**, *4*, 348–356.
- (28) Truong, P. V.; Shingleton, S.; Kammoun, M.; Black, R. L.; Charendoff, M.; Willis, C.; Ardebili, H.; Stein, G. E. Structure and Properties of Sulfonated Pentablock Terpolymer Films as a Function of Wet-Dry Cycles. *Macromolecules* **2018**, *51*, 2203–2215.
- (29) Zhang, Y.; Batys, P.; O'Neal, J. T.; Li, F.; Sammalkorpi, M.; Lutkenhaus, J. L. Molecular Origin of the Glass Transition in Polyelectrolyte Assemblies. ACS Cent. Sci. 2018, 4, 638–644.
- (30) Nolte, A. J.; Treat, N. D.; Cohen, R. E.; Rubner, M. F. Effect of relative humidity on the Young's modulus of polyelectrolyte multilayer films and related nonionic polymers. *Macromolecules* **2008**, *41*, 5793–5798.
- (31) Hariri, H. H.; Lehaf, A. M.; Schlenoff, J. B. Mechanical properties of osmotically stressed polyelectrolyte complexes and multilayers: Water as a plasticizer. *Macromolecules* **2012**, *45*, 9364–9372.
- (32) Zhang, Y.; Li, F.; Valenzuela, L. D.; Sammalkorpi, M.; Lutkenhaus, J. L. Effect of water on the thermal transition observed in poly(allylamine hydrochloride)-poly(acrylic acid) complexes. *Macromolecules* **2016**, *49*, 7563–7570.
- (33) Choi, J. H.; Willis, C. L.; Winey, K. I. Structure-property relationship in sulfonated pentablock copolymers. *J. Membr. Sci.* **2012**, 394-395, 169–174.
- (34) Suarez-Martinez, P. C.; Batys, P.; Sammalkorpi, M.; Lutkenhaus, J. L. Time-Temperature and Time-Water Superposition Principles Applied to Poly(allylamine)/Poly(acrylic acid) Complexes. *Macromolecules* **2019**, *52*, 3066–3074.

- (35) Zhang, R.; Zhang, Y.; Antila, H. S.; Lutkenhaus, J. L.; Sammalkorpi, M. Role of salt and water in the plasticization of PDAC/PSS polyelectrolyte assemblies. *J. Phys. Chem. B* **2017**, *121*, 322–333.
- (36) Kreuer, K.-D.; Paddison, S. J.; Spohr, E.; Schuster, M. Transport in Proton Conductors for Fuel-Cell Applications. *Chem. Rev.* **2004**, *104*, 4637–4678.
- (37) Willis, C. L.; Handlin, D. L.; Trenor, S. R.; Mather, B. D. Sulfonated block copolymers, method for making same, and various uses for such block copolymers. *United States Patent Application*, US 2007/0,021,569 A1, 2007.
- (38) Williams, D. B. G.; Lawton, M. Drying of Organic Solvents: Quantitative Evaluation of the Efficiency of Several Desiccants. *J. Org. Chem.* **2010**, *75*, 8351–8354.
- (39) Patterson, A. L. The scherrer formula for X-ray particle size determination. *Phys. Rev.* **1939**, *56*, 978–982.
- (40) Buzzoni, R.; Bordiga, S.; Ricchiardi, G.; Spoto, G.; Zecchina, A. Interaction of H2O, CH3OH, (CH3)2O, CH3CN, and pyridine with the superacid perfluorosulfonic membrane nation: An IR and Raman study. *J. Phys. Chem.* **1995**, *99*, 11937–11951.
- (41) Huang, H.; Hu, Z.; Chen, Y.; Zhang, F.; Gong, Y.; He, T.; Wu, C. Effects of casting solvents on the formation of inverted phase in block copolymer thin films. *Macromolecules* **2004**, *37*, 6523–6530.
- (42) Zhang, Q.; Tsui, O. K. C.; Du, B.; Zhang, F.; Tang, T.; He, T. Observation of inverted phases in poly(styrene-b-butadiene-b-styrene) triblock copolymer by solvent-induced order-disorder phase transition. *Macromolecules* **2000**, *33*, 9561–9567.
- (43) Huang, H.; Zhang, F.; Hu, Z.; Du, B.; He, T.; Lee, F. K.; Wang, Y.; Tsui, O. K. C. Study on the origin of inverted phase in drying solution-cast block copolymer films. *Macromolecules* **2003**, *36*, 4084–4092.
- (44) Radjabian, M.; Abetz, C.; Fischer, B.; Meyer, A.; Abetz, V. Influence of Solvent on the Structure of an Amphiphilic Block Copolymer in Solution and in Formation of an Integral Asymmetric Membrane. ACS Appl. Mater. Interfaces 2017, 9, 31224–31234.
- (45) Modi, A.; Bhaway, S. M.; Vogt, B. D.; Douglas, J. F.; Al-Enizi, A.; Elzatahry, A.; Sharma, A.; Karim, A. Direct Immersion Annealing of Thin Block Copolymer Films. *ACS Appl. Mater. Interfaces* **2015**, *7*, 21639–21645.